Journal of Experimental Botany, Vol. 70, No. 14 pp. 3679–3691, 2019
doi:10.1093/jxb/erz286 Advance Access Publication 13 July, 2019

RESEARCH PAPER

Mechanical properties and structure–function trade-offs in secondary xylem of young roots and stems

Lenka Plavcová[1,*], Friederike Gallenmüller[2], Hugh Morris[3], Mohammad Khatamirad[4], Steven Jansen[4] and Thomas Speck[2,5]

[1] University of Hradec Králové, Department of Biology, Faculty of Science, Rokitanského 62, 500 03 Hradec Králové, Czech Republic
[2] Plant Biomechanics Group Freiburg, Botanic Garden of the Albert-Ludwigs-University of Freiburg, Faculty of Biology, Schänzlestrasse 1, 79104 Freiburg, Germany
[3] Laboratory for Applied Wood Materials, Empa – Swiss Federal Laboratories for Materials Testing and Research, St Gallen, Switzerland
[4] Institute of Systematic Botany and Ecology, Ulm University, Albert-Einstein-Allee 11, D-89081 Ulm, Germany
[5] Cluster of Excellence livMatS @ FIT – Freiburg Center for Interactive Materials and Bioinspired Technologies, Georges-Köhler-Allee 105, 79110 Freiburg, Germany

* Correspondence: lenka.plavcova@gmail.com

Received 14 December 2018; Editorial decision 3 June 2019; Accepted 27 June 2019

Editor: Anja Geitmann, McGill University, Canada

Abstract

Bending and torsional properties of young roots and stems were measured in nine woody angiosperms. The variation in mechanical parameters was correlated to wood anatomical traits and analysed with respect to the other two competing functions of xylem (namely storage and hydraulics). Compared with stems, roots exhibited five times greater flexibility in bending and two times greater flexibility in torsion. Lower values of structural bending and structural torsional moduli (E_{str} and G_{str}, respectively) of roots compared with stems were associated with the presence of thicker bark and a greater size of xylem cells. Across species, E_{str} and G_{str} were correlated with wood density, which was mainly driven by the wall thickness to lumen area ratio of fibres. Higher fractions of parenchyma did not translate directly into a lower wood density and reduced mechanical stiffness in spite of parenchyma cells having thinner, and in some cases less lignified, cell walls than fibres. The presence of wide, partially non-lignified rays contributed to low values of E_{str} and G_{str} in *Clematis vitalba*. Overall, our results demonstrate that higher demands for mechanical stability in self-supporting stems put a major constraint on xylem structure, whereas root xylem can be designed with a greater emphasis on both storage and hydraulic functions.

Keywords: Axial parenchyma, fibres, mechanical function, rays, structural bending modulus, structural torsional modulus, trade-off, wood.

Introduction

Wood fulfils several biophysical functions, including the facilitation of long-distance transport of water and nutrients (Tyree and Ewers, 1991), mechanical support (Badel *et al.*, 2015), and storage of water (Tyree and Yang, 1990), nutrients (Plavcová *et al.*, 2016) and secondary compounds (Morris *et al.*, 2016*a*). In most angiosperms, these functions are seemingly divided between different cell types.Vessels and tracheids are specialised in the hydraulic function, fibres are devoted to mechanical support, whereas ray and axial parenchyma act as the main sites for storage and movement of non-structural carbohydrates.

© The Author(s) 2019. Published by Oxford University Press on behalf of the Society for Experimental Biology. All rights reserved.
For permissions, please email: journals.permissions@oup.com

Downloaded from https://academic.oup.com/jxb/article-abstract/70/14/3679/5531920 by Lib4RI Empa user on 03 September 2019

However, this view is to a certain degree oversimplified because the different cell types and the functions commonly attributed to them are in fact tightly interwoven and linked in a complex manner. The interaction between mechanical and hydraulic function arises because structural support from fibres helps to prevent hydraulic dysfunction (Jacobsen *et al*., 2005; Lens *et al*., 2016) and bridges made out of pitted fibre–tracheids hydraulically connect isolated vessels thereby serving as a safer auxiliary pathway for water transport (Cai *et al*., 2014). Similarly, parenchyma cells, which are primarily devoted to nutrient storage, may interact with hydraulic function by facilitating embolism reversal (Brodersen *et al*., 2010) and by providing hydraulic capacitance (Pfautsch *et al*., 2015). The storage and mechanical function is also interlinked as ray parenchyma affects wood mechanical strength (Burgert *et al*., 2001) and living fibres are involved in storage of non-structural carbohydrates in some species (Yamada *et al*., 2011). Thus, determining to what degree multiple functions overlap in wood and deciphering the key anatomical drivers associated with physiological traits remains a challenge.

When analysing relationships in xylem structure and function, ecologists have frequently viewed traits as being along contrasting spectra of trade-offs (Baas *et al*., 2004; Pratt and Jacobsen, 2017). Several structural–functional trade-offs have already been described in wood, although the continuum and multi-functionality of xylem tissue is unlikely to be simplified to strictly opposing categories. The covariation between hydraulic safety versus efficiency is one of the most frequently studied relationships, although this apparent trade-off remains fairly weak and poorly understood (Lens *et al*., 2011; Bittencourt *et al*., 2016; Gleason *et al*., 2016). Also, the strength of the trade-off may vary between different growth forms (van der Sande *et al*., 2019). A trade-off between hydraulic and mechanical function is another example of structure–function relationships, which has been documented at cellular and tissue levels. The existence of a trade-off between hydraulics and mechanics is more self-evident in conifers because tracheids fulfil both of these functions. Across a wide range of conifer species, higher mechanical reinforcement of tracheids was associated with increased hydraulic resistance (Pittermann *et al*., 2006). The trade-off arose from cell reinforcement primarily achieved by narrowing of cell diameters rather than through increase in the thickness of the secondary wall. In angiosperms, hydraulic and mechanical functions can be more easily decoupled because of the distinct roles of vessels and fibres. Thus, hydraulic conductivity can theoretically remain unchanged in mechanically stronger wood if the increased mechanical strength is achieved by modifying fibre properties. In agreement, no significant relationship between mechanical strength and hydraulic conductivity was observed across five *Acer* species in which higher mechanical strength was due to the presence of narrower fibre lumen diameters (Woodrum *et al*., 2003). However, a strong negative correlation between specific hydraulic conductivity and the modulus of elasticity was reported along the root axial length in six tropical tree species (Christensen-Dalsgaard *et al*., 2007*a*,*b*). In this case, changes in wood density corresponded with a strong gradient in the size and frequency of vessels. Thus, while there is evidence for the negative coupling between hydraulics and mechanics in both gymnosperms and at least some angiosperm species, a trade-off between mechanical and storage functions has rarely been considered beyond the observation of a negative correlation between fibre and parenchyma fractions (Pratt *et al*., 2007; Zieminńska *et al*., 2015; Morris *et al*., 2016*b*).

The evolution of secondary growth and production of secondary xylem (i.e. wood) can be considered one of the strategies increasing the mechanical stability of plants, allowing for larger and taller plant bodies. Resistance of woody organs to mechanical loads can be correlated to complex morpho-anatomical structures at different hierarchical levels (Speck and Burgert, 2011; Lachenbruch and McCulloh, 2014). The character and intensity of the dominant stresses and strains change along the plant body. Therefore, mechanical properties of wood vary considerably within one individual and also along one individual root or stem (Niklas, 1999*b*, Christensen-Dalsgaard *et al*., 2007*a*). High mechanical stiffness of wood has been repeatedly linked to high wood density (Jacobsen *et al*., 2007; Niklas and Spatz, 2010). However, it is often less clear which finer-scale anatomical properties are the main drivers of this integrative trait (Ziemińska *et al*., 2013). While fibre properties certainly exert strong control over wood density and wood mechanical properties (Fujiwara *et al*., 1991; Jacobsen *et al*., 2007), considerable influence of ray and axial parenchyma has also been reported across a diverse range of species (Fujiwara, 1992; Zheng and Martínez-Cabrera, 2013; Ziemińska *et al*., 2015). A high proportion of thin-walled parenchyma cells occurring at the expense of thick-walled fibres is expected to lead to a reduction in wood mechanical stiffness. However, the mechanical effects are hypothesised to differ between ray and axial parenchyma, partly owing to their orientation in radial and axial directions (Zheng and Martínez-Cabrera, 2013). Due to the perpendicular orientation of rays to the wood grain, a high proportion of them were found to enhance the mechanical stiffness of wood, particularly in the radial direction (Burgert *et al*., 2001; Woodrum *et al*., 2003). Contrarily, it has been suggested that the presence of wide rays underpins a high torsional and flexural flexibility of liana stems (Gartner, 1991; Putz and Holbrook, 1991; Carlquist, 2001). In comparison to ray parenchyma, axial wood parenchyma cells are grouped in strands that have a similar shape and longitudinal orientation to fibres. Therefore, a higher proportion of axial parenchyma should directly reduce the stiffness of the fibre matrix. However, several questions have not been fully addressed yet, such as (i) to what extent the amount of parenchyma can have an appreciable effect on wood stiffness, and (ii) whether the relative differences in wall reinforcement between axial wood parenchyma and fibres are similar across species and organs.

In the current study, we measured bending and torsional moduli and conducted detailed observations of wood anatomy of young stems and roots in nine angiosperm species. The main objectives of our study were (i) to evaluate the effect of ray and axial parenchyma on mechanical properties and (ii) to better understand the trade-offs in xylem structure–function. Young stems and roots provide a convenient study system for this purpose as these organs are designed with a different adaptive emphasis on mechanical, storage, and hydraulic functions. We

Downloaded from https://academic.oup.com/jxb/article-abstract/70/14/3679/5531920 by Lib4RI Empa user on 03 September 2019

expected self-supporting stems to be mechanically stronger than roots, but the question arose as to whether hydraulics or storage or both of these functions are consequently increased in roots. Furthermore, we anticipated morphological and anatomical features that presumably underlie a higher mechanical stiffness (e.g. less abundant axial wood parenchyma, narrower rays, and thicker cell walls) to be more prominent in stems as opposed to roots.

Materials and methods

Plant material

Young roots and stems were collected from nine different angiosperm species, including eight common temperate forest trees, and one temperate woody liana (Table 1). The latter was included in our comparative study, to get some first results on differences in functional trade-offs between self-supporting angiosperm trees and non-self-supporting lianas. All samples were collected from a minimum of three mature individuals per species during June to August 2014. The sampling was done in a forested area of the Ulm University campus (48° 25′N, 9° 58′E), from a forest strip along the Iller river 2 km south of Ulm (48° 22′N, 9° 60'E), and in a forested area located 4 km southeast of Freiburg, Germany (47° 59′N, 7° 53′E). The root segments were excavated from 10–50 cm depth in a distance of approx. 1 m from the root collar. The stem segments were cut from lateral branches at a height of 2–3 m with the aid of a telescopic pruning pole. The diameters of the segments ranged between 0.5 to 1.5 cm and their ages were between 3 and 8 years. All segments had already undergone substantial secondary thickening but still can be classified as juvenile in relation to the age of the plant specimens they were collected from. Thus, the sampled segments had morphological and anatomical characteristics typical of root and stem organs and could be considered, based on their age and position in the entire plant body, as being in the medium advance in their specialisation process towards mechanical, hydraulic, and storage demands. Upon collection, the samples were put into a dark plastic bag with a moist paper towel and transported to the laboratory where they were stored at 4 °C until used for mechanical measurements. All samples were measured within 3 days of collection.

Table 1. *List of abbreviations*

Abbreviation	
Species	
Ap	*Acer pseudoplatanus* L.
Cb	*Carpinus betulus* L.
Fe	*Fraxinus excelsior* L.
Fs	*Fagus sylvatica* L.
Pa	*Prunus avium* (L.) L.
Qr	*Quercus robur* L.
Rp	*Robinia pseudoacacia* L.
Tc	*Tilia cordata* Mill.
Cv	*Clematis vitalba* L.
Organs	
R	Roots
S	Stems
Mechanical parameters	
EI	Bending stiffness (N m^2)
GI	Torsional stiffness (N m^2)
E_{str}	Structural bending modulus (MN m^{-2})
G_{str}	Structural torsional modulus (MN m^{-2})
I_{ax}	Axial second moment of area (m^4)
I_{pol}	Polar second moment of area (m^4)
$I_{rel,tissue}$	Relative contribution of tissue (wood, bark, or pith) to I_{ax} or I_{pol}

Flexural and torsional stiffness

Mechanical measurements were performed on stem and root segments with a length of 10–25 cm. Care was taken to select straight segments with a low degree of taper, avoiding side branches, knots, and obvious structural damage. Flexural stiffness was measured in four-point-bending tests using a manual bending apparatus. The segments were placed on two cylindrical holders 5–12 cm apart from each other, depending on the length and the bending resistance of the tested segment. The bending force was applied via a suspended holder, which was attached to the tested sample at two points, and placed equidistant and outside of the cylindrical supports. The bending force was then gradually increased by adding up to six weights of 50, 100, or 200 g onto the metal holder. The resulting upward deflection of the segment was monitored with an eyepiece graticule on a dissecting microscope. The cumulative deflection values were plotted against the applied force and fitted with a linear equation. Only measurements with a coefficient of determination higher than 0.97 were accepted. The flexural stiffness (EI) was then calculated as

$$EI = \frac{l_1^2 \times \frac{1}{2}(l_2 - l_1)}{16 \times a} \quad (1)$$

where l_1 is the distance of the sample holders (i.e. support span, in m), l_2 is the span of the weight holder attachment (i.e. load span, in m) and a is the slope of the linear regression line of the deflection versus applied force data (in N m^{-1}). For a detailed description of the bending tests and formulas see Niklas (1992), Speck (1994), Rowe and Speck (1996), and Rowe *et al.* (2006).

The flexural stiffness is determined by the dimensions of a sample (described by the axial second moment of area, I_{ax}) and its material properties (described by the structural bending modulus, E_{str}), according to the following formula:

$$EI = E_{str} I_{ax} \quad (2)$$

In engineering, the term bending modulus is defined as a property of a homogeneous and isotropic material. As plant stems and roots are heterogeneous, anisotropic composite structures, we use the term *structural* bending modulus E_{str} (Rowe and Speck, 1996; Speck *et al.*, 1996). The higher the resistance to bending or tension of a sample, the higher is its structural modulus of elasticity, independent of its geometrical dimensions (Niklas, 1992). Following Eq. 2, the structural bending modulus E_{str} was obtained by dividing the flexural stiffness EI by I_{ax}, with I_{ax} being calculated according to the following formula:

$$I_{ax} = \frac{\pi}{64} D^4 \quad (3)$$

where D is the root or stem diameter (in m). The diameter was obtained from the measured mean cross-sectional area of the tested root or stem when assuming a circular geometry. Due to the fact that the stems and roots segments tested in our study showed almost perfectly circular cross-sections and small deviations were developed only intermittently and never along the whole segment, we decided that the use of a circular model represents the best approximation.

Immediately after the bending test, which was limited to the elastic range of the samples, torsional stiffness was assessed on the same root or stem segment. The torsional stiffness was measured using a range of custom-made spring-loaded cylinders that could apply a range of torques according to the thickness and resistance of the samples tested. The torsion cylinders consist of a central spindle and a clamp that can rotate freely against a spring. The cylinder was gradually rotated in 10–20° steps against the spring. The resulting root or stem deflection was measured relative to the torsional force applied. Torque was calculated by multiplying the rotational angle with the stiffness of the spring inside the cylinder determined from a calibration curve. Torsional stiffness (GI) was then calculated by dividing the length of the tested segment (l, in m) by the slope of the regression line fitted to the data of deflection angles plotted against the applied torque (b, in rad N^{-1} m^{-1}), according to the following formula:

$$GI = \frac{l}{b} \quad (4)$$

Downloaded from https://academic.oup.com/jxb/article-abstract/70/14/3679/5531920 by Lib4RI Empa user on 03 September 2019

The structural torsional modulus was calculated using the formula:

$$G_{str} = \frac{GI}{I_{pol}} \quad (5)$$

where I_{pol} is the polar second moment of area of the tested segment calculated as:

$$I_{pol} = \frac{\pi}{32} D^4 \quad (6)$$

where D represents the mean root or stem diameter (i.e. assuming circular geometry of the tested segments, same as for I_{ax}). For a detailed description of the torsional tests see Gallenmüller *et al.* (2001).

Tissue proportions and their contribution to I_{ax} and I_{pol}

Roots and stems are highly inhomogeneous and anisotropic structures composed of different tissues, namely wood and bark in the case of roots, and pith, wood, and bark in the case of stems. To gain insights into the relative importance of these three tissues for the overall mechanical stiffness, their relative contributions to I_{ax} and I_{pol} were assessed. To calculate the relative contribution of each tissue to I_{ax} and I_{pol} ($I_{rel,tissue}$), the cross-sectional areas of pith, wood, and bark were measured from surface images of stem cross-sections obtained with a stereo zoom microscope (Axio Zoom V16, Zeiss, Germany). In roots, which do not have pith tissue, only the relative contribution of wood and bark was considered. The tissue cross-sectional areas were then converted to diameters and the partial second moments of area ($I_{ax,tissue}$ and $I_{pol,tissue}$) of each tissue were calculated assuming circular tissue outlines and a symmetrical distribution. The standard formulas for filled cylinders (Eqs 5, 6) were used to calculate the partial second moment of area of wood in roots and pith in young stems, whereas the partial second moment of area of bark in both stems and roots and of wood in stems was derived using standard formulas for hollow cylinders:

$$I_{ax,\ tissue} = \frac{\pi}{64}\left(D_j^4 - D_i^4\right)$$

, and correspondingly

$$I_{pol,\ tissue} = \frac{\pi}{32}\left(D_j^4 - D_i^4\right)$$

where D_j and D_i are outer and inner diameters of the tissue outlines. The relative contribution of each tissue to I_{ax} and I_{pol} ($I_{rel,tissue}$) was finally calculated by dividing $I_{ax,tissue}$ ($I_{pol,tissue}$) by I_{ax} (I_{pol}). As the relative contributions of the different tissues are equal for I_{ax} and I_{pol}, the $I_{rel,tissue}$ values are not reported separately for axial and polar moments of area.

Wood traits

Wood density (in g cm^{-3}) was measured using the water displacement method. Root and stem segments, about 3 cm in length, were cut and debarked. Stem segments were additionally split in half and the pith carefully removed. The wood pieces were soaked in water for at least 30 min to ensure they were well hydrated. Each segment was then immersed into a water-filled beaker placed on an electronic balance with the aid of a dissecting needle and the weight of the displaced water was recorded. All segments were then dried at 80 °C for 24 h to a constant weight, and wood density was calculated by dividing the wood dry weight by the volume of displaced water.

For wood anatomical measurements, transverse sections about 40 µm thick were prepared with a sliding microtome. The sections were stained in a mixture of 0.35% safranin and 0.65% alcian blue, dehydrated through an ethanol series, and mounted in Neo-Mount (Merck Millipore, Germany). The relative proportions of various cell types in wood, i.e. vessels, fibres (including tracheids), and ray and axial parenchyma, were measured with an Axio Zoom V16 microscope on wedge-shaped transects spanning from the root or stem centre to the cambium at ×150 magnification. Image analysis involved manual tissue segmentation in Photoshop followed by area proportion measurements using Fiji/ImageJ (Schindelin *et al.*, 2012). To obtain the relative proportions of different cell types, the total surface area taken up by each cell type was divided by the total surface area of the entire transect measured. The axial and ray parenchyma proportions were already published in Plavcová *et al.* (2016).

In addition to cell type proportions, finer scale anatomical parameters were analysed. Vessel lumen area was measured on the same xylem wedges as the cell type proportions. The lumen areas were converted to vessel diameters assuming circular vessel geometry. Ray density was measured by counting the number of rays per quarter-circle-shaped root or stem wedge imaged at ×100 magnification. Ray width was assessed on images taken at ×200 magnification. The double wall thickness (DWT) and the lumen area of fibres and axial parenchyma cells were measured on transverse sections. These measurements were done at ×1000 magnifications using a light microscope equipped with an oil immersion objective (Leitz DMRB, Leica, Germany). At least 150 individual cells were measured for each species and organ. The lumen area was converted to lumen diameter (D_L) assuming a circular cell shape and the cell cross-sectional area (CSA), including the cell lumen and secondary wall, was calculated as $\pi(D_L/2+DWT/2)^2$. In addition, the thickness to span ratio of fibre and axial parenchyma was calculated by dividing DWT by D_L, and used as a measure of cell reinforcement (Pittermann *et al.*, 2006). The DWT and CSA values for four out of the nine species shown here were already published in Jupa *et al.* (2016).

Wood density and wood anatomy measurements were carried out on a different set of samples from those used for the mechanical testing. However, the samples were collected from the same population of trees following the same sampling scheme. Wood density was measured for six root and stem samples from at least three different individuals per species. Wood anatomy was measured on three root and stem samples from three different individuals.

Carbohydrate storage capacity and hydraulic conductivity of wood

In addition to data on mechanical properties, we obtained estimates of wood storage capacity and hydraulic conductivity in order to analyse potential trade-offs among the three competing functions. Concentrations of non-structural carbohydrates (NSC) in root wood and stem wood (in mg g^{-1}) measured for the same population of trees were taken from Plavcová *et al.* (2016), and used as a measure of wood storage capacity. Theoretical hydraulic conductivity was calculated from the measured vessel radius (r) using the Hagen–Poiseuille equation ($K_h=(\pi r^4)/8\mu$) and normalized by a corresponding xylem wedge area (McCulloh *et al.*, 2010). All three functional parameters (E_{str}, NSC, and K_h) were then converted to a common scale from 0 to 100 and plotted on ternary axes using the ggtern R package (Hamilton and Ferry, 2018).

Statistical analyses

The differences in structural and functional parameters between roots and stems were analysed using linear mixed-effect models. The models were fitted with organ (root or stem) being considered as a fixed factor and species identity as a random factor. To analyse differences in cell wall thickness of fibres and axial parenchyma, cell type was implemented as an additional fixed effect factor. Prior to the modelling, the normality and homogeneity of variance of the data were checked using the Shapiro–Wilk and Bartlett's tests, respectively. When the assumptions were not met, the data were log transformed. The analyses were conducted on species-level means. The models were fitted using the lme function from the nlme R package (Pinheiro *et al.*, 2013). The mixed effect models described above were designed to test for the overall difference between the two organs across all species. In addition, we analysed differences between roots and stems within each species using the Welch two-sample *t*-test. The interspecific differences in mechanical parameters within each organ were evaluated using Tukey-adjusted multiple mean comparisons. All data analyses were completed using R statistical software (R Core Team, 2016).

Results

Mechanical properties

On average, roots were about five times more flexible in bending and two times more flexible in torsion than stems.

Downloaded from https://academic.oup.com/jxb/article-abstract/70/14/3679/5531920 by Lib4RI Empa user on 03 September 2019

The total axial second moment of area (I_{ax}) fell in a relatively narrow range of between 100 and 250 mm^4 for most of the samples measured as care was taken to collect samples of similar diameter. Correspondingly, the total polar second moment of area (I_{pol}) values ranged between 150 and 550 mm^4. Slightly larger stems and roots, corresponding to I_{ax} and I_{pol} values of ca. 500 mm^4 and 1000 mm^4, respectively, were collected for the woody climber *Clematis vitalba*. When structural bending and structural torsional moduli (E_{str} and $G_{str,}$) were calculated, neither of them correlated significantly with I_{ax} and I_{pol} ($P>0.05$). Thus, we assume that the variation of E_{str} and G_{str} occurring during ontogeny can be neglected in good approximation within the range of sample size tested in this study.

E_{str} and G_{str} values varied substantially among species and organs, with E_{str} ranging from 558 to 2913 MN m^{-2} and from 1220 to 12 681 MN m^{-2} (Fig. 1A) and G_{str} spanning from 48 to 254 MN m^{-2} and from 50 to 532 MN m^{-2} (Fig. 1B) for roots and stems, respectively. *Carpinus betulus* showed the highest E_{str} and G_{str} measured among all roots, while the roots of *Robinia pseudoacacia* were found to be the most flexible. Among stems, *Robinia pseudoacacia*, *Carpinus betulus*, *Acer pseudoplatanus*, *Fraxinus excelsior*, and *Fagus sylvatica* exhibited high values of both E_{str} and G_{str}, whereas the stems of *Clematis vitalba*, *Tilia cordata*, and *Quercus robur* showed relatively low resistance to deformation in both bending and twisting (Fig. 1). Neither E_{str} nor G_{str} showed a significant linear correlation between roots and stems ($P>0.05$), indicating that the mechanical properties of roots and stems within the same species are rather independent of each other. Contrasting mechanical properties of roots and stems were most apparent in *Robinia pseudoacacia*. Furthermore, all samples measured were consistently stiffer in bending than in torsion, as shown by their twist to bend ratios (EI/GI) higher than 1. Roots had significantly lower bend to twist ratios than stems (Fig. 1C). Overall, E_{str} and G_{str} values were closely correlated across species and organs (Fig. 2A, $r^2=0.77$, $P<10^{-4}$ and $r^2=0.86$, $P<10^{-4}$ for roots and stems, respectively).

Relative tissue contributions to axial and polar second moment of area

The mean relative contribution of pith to I_{ax} or I_{pol} ($I_{rel,pith}$) was very small in all stems measured, with $I_{rel,pith}$ typically less than 0.01 and never over 0.05. The mean relative contribution of wood to I_{ax} or I_{pol} ($I_{rel,wood}$) was 0.36 in roots and 0.48 in stems. Thus, the relative contribution of bark ($I_{rel,bark}$) was 12% higher in roots than in stems. Substantial differences in $I_{rel,wood}$ and $I_{rel,bark}$ also existed across the species investigated. The stems of *Carpinus betulus*, *Fagus sylvatica*, *Robinia pseudoacacia*, and *Acer pseudoplatanus* showed $I_{rel,wood}$ higher than 0.5, whereas $I_{rel,wood}$ values lower than 0.4 were observed in the stems of *Clematis vitalba* and *Tilia cordata*. Due to the presence of a thick bark, $I_{rel,wood}$ was also relatively low (i.e. less than 25%) in *Robinia pseudoacacia* and *Fraxinus excelsior* roots. In contrast, the roots of *Fagus sylvatica* had a very thin bark and hence $I_{rel,wood}$ was as high as 59%. In both organs, a higher proportion of wood was associated with higher mechanical stiffness, as indicated by significant positive correlations between $I_{rel,wood}$ and both E_{str} (Fig. 2B, $r^2=0.62$, $P<0.05$ and $r^2=0.81$, $P<10^{-4}$ for roots and stems, respectively) and G_{str} ($r^2=0.65$, $P<0.01$ and $r^2=0.91$, $P<10^{-4}$ for roots and stems, respectively).

Xylem anatomical traits in relation to mechanical properties

Wood density was significantly correlated with both E_{str} ($r^2=0.27$, $P<0.05$) and G_{str} ($r^2=0.33$, $P<0.05$) when data from the two organs were pooled. When the organs were considered separately, a significant correlation was found only between wood density and E_{str} in roots ($r^2=0.48$, $P=0.04$, Fig. 2C). Fibre properties appeared to be the main driver of wood density as evidenced by a significant positive correlation with fibre double wall thickness to lumen diameter ratio (referred to as fibre thickness to span ratio hereafter, Fig. 2D). The tissue fractions of ray and axial wood parenchyma did not correlate significantly with the mechanical parameters and were not directly associated with wood density ($P>0.05$). The cell walls of both axial parenchyma and fibres were lignified as evidenced by staining with safranin. However, compared with fibres, axial wood parenchyma showed similar cross-sectional areas (Fig. 3A) and narrower cell walls than fibres (Fig. 3B), leading to a lower thickness to span ratio in axial wood parenchyma of both roots and stems (Fig. 3C). On the contrary, comparison of cell lumen and cell wall dimensions between organs revealed significantly higher mean cross-sectional areas in roots than in stems (Fig. 3A), but a similar mean cell wall thickness in both axial wood parenchyma and fibres (Fig. 3B). However, the resulting tendency to lower thickness to span ratios in roots compared with stems was not statistically significant (Fig. 3C). Across species, the thickness to span ratios of axial parenchyma cells were more homogeneous, ranging from 0.13 to 0.24 in roots and from 0.16 to 0.37 in stems, while the thickness to span ratios of fibres were much more variable, ranging from 0.15 to 1.09 in roots and from 0.17 to 0.79 in stems (Fig. 4). The interspecific variation in the thickness to span ratio was primarily determined by the wall thickness rather than the cell diameter as evidenced by approximately two times higher coefficients of covariation between thickness to span ratio and wall thickness.

Roots had wider rays ($P=0.01$) and higher overall fractions of radial parenchyma ($P=0.004$) compared with stems. However, wide rays were not universally associated with greater mechanical flexibility. For instance, wide multiseriate rays were found in both stems and roots of *Fagus sylvatica* (Fig. 5A, B, E, F), although these organs belonged to the mechanically stiffest specimens. In most species, ray cell walls were as thick as fibre walls and appeared lignified as indicated by a positive staining reaction with safranin. *Clematis vitalba* represented the only notable exception from this general pattern. In this species, the outermost portions of rays in both roots and stems were non-lignified as evidenced by intensive staining with alcian blue (Fig. 5H).

Association between traits and trade-off analysis

A principal component analysis (PCA) clearly separated roots and stems, summarized correlations between multiple traits,

Downloaded from https://academic.oup.com/jxb/article-abstract/70/14/3679/5531920 by Lib4RI Empa user on 03 September 2019

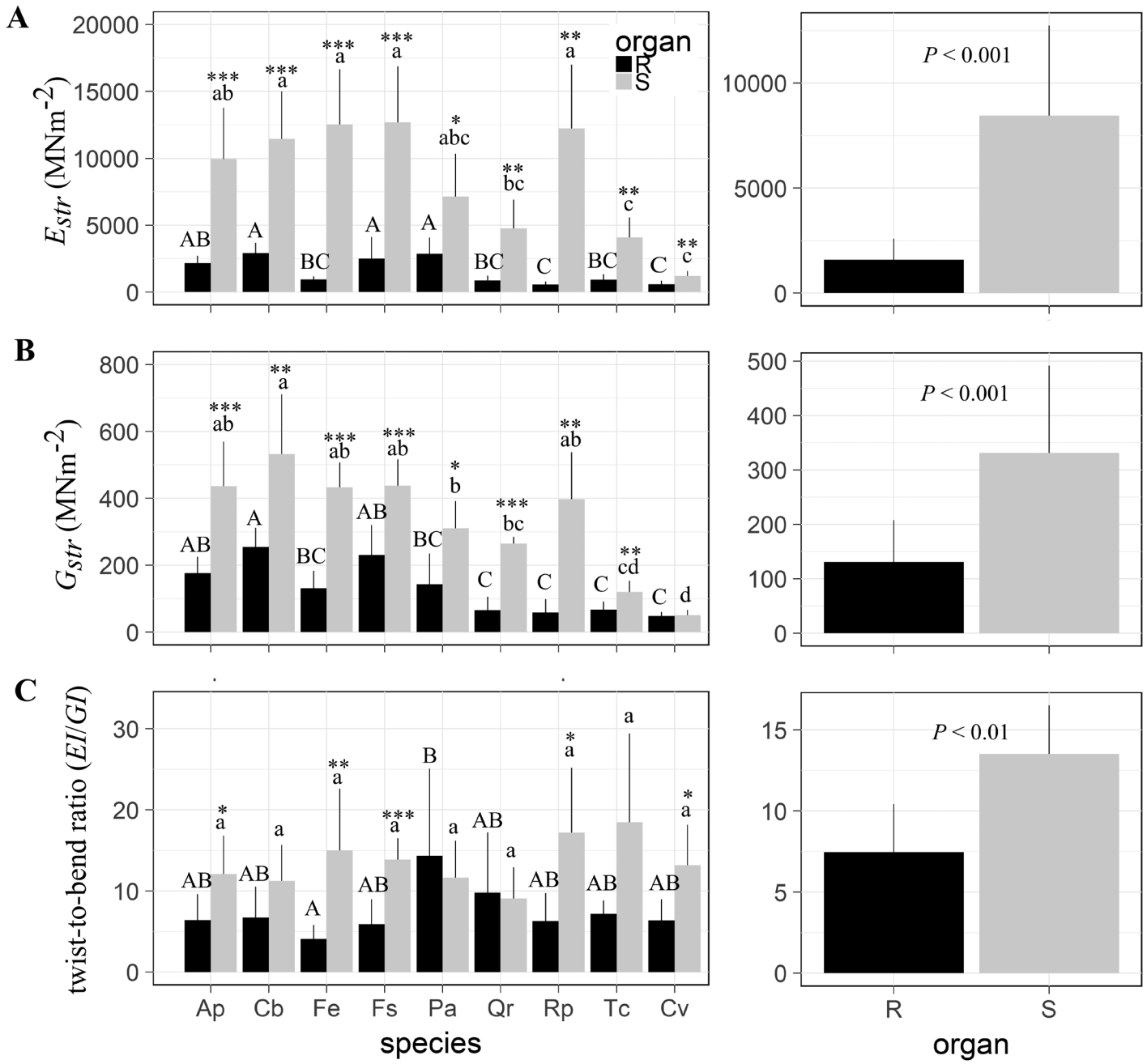

Fig. 1. Mechanical properties of young woody roots and stems. Structural bending moduli (E_{str}) (A), structural torsional moduli (G_{str}) (B) and ratios between bending and torsional stiffness (*EI*/*GI*) (C) in roots (R) and stems (S) of nine woody angiosperms. Bars represent species-level means ±SD (left-hand graph panels, *n*=6–8 samples) and root- and stem-level means ±SD calculated from the species-level means (right-hand panels, *n*=9 species). Roots and stems are depicted in black and grey, respectively. For abbreviation of species names see Table 1. Asterisks above bars indicate significant differences between root and stems within each species (Welch two sample *t*-test) at $P<0.05$ (*), $P<0.01$ (**) and $P<0.001$ (***). Significant differences between species within each organ are indicated by different letters (Tukey's adjusted multiple mean comparisons); uppercase letters are for roots, lowercase letters are for stems. *P*-values in the right-hand panels correspond to significance levels of the fixed effect 'organ' (mixed effect models with random effect of species).

and provided insights into trade-offs and their structural underpinnings (Fig. 6). The first component explained 45% of the variation of the dataset and showed strong positive loadings with E_{str}, G_{str}, $I_{xyl.rel}$, and wood density, and negative loadings with lumen area of parenchyma cells and vessel diameter. The first component can therefore be interpreted as a trade-off between mechanical function, which is prominent in stems, and storage and hydraulic functions that are both more emphasized in roots. The second component, which explained 22% of the variation, was most strongly related to fibre and parenchyma tissue fractions, which co-vary in the opposite direction.

The overall coordination between mechanical stiffness, storage capacity, and hydraulic conductivity was also visualized in ternary diagrams. The diagrams provide evidence for structure–functional trade-offs that differ across and within organs (Fig. 7). A strong trade-off between mechanical

Downloaded from https://academic.oup.com/jxb/article-abstract/70/14/3679/5531920 by Lib4RI Empa user on 03 September 2019

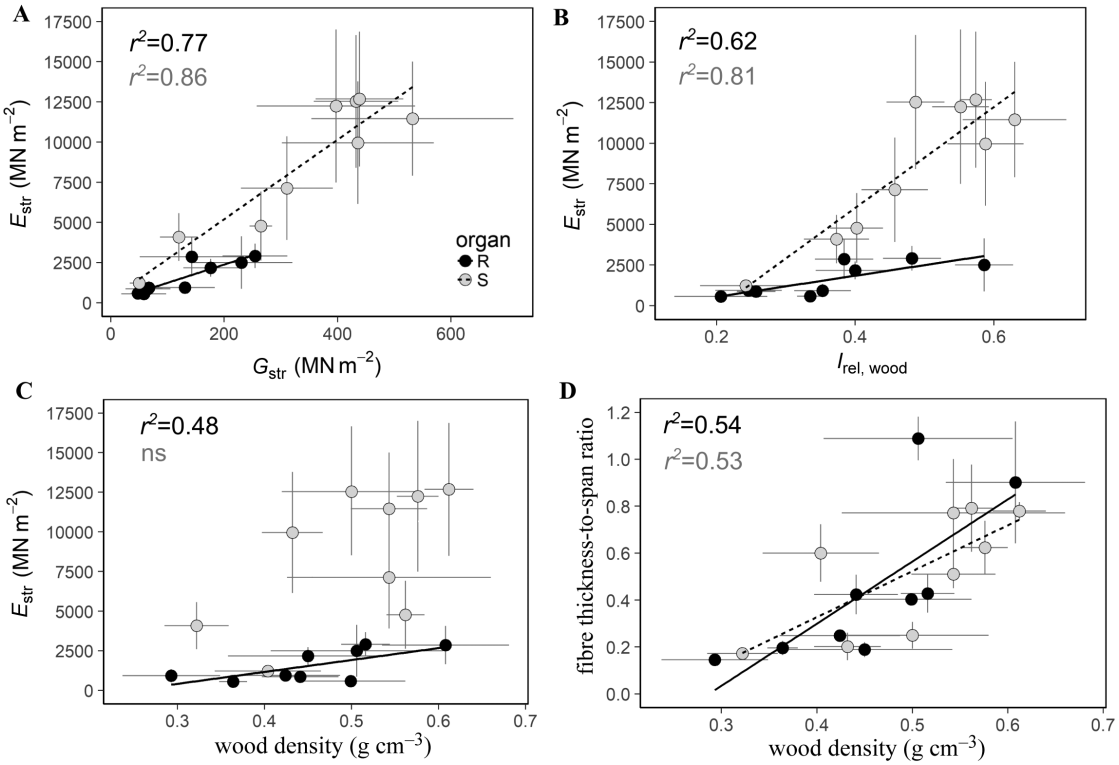

Fig. 2. Correlations between mechanical and structural properties. Correlation between (A) structural bending modulus (E_{str}) and structural torsional modulus (G_{str}), (B) between the contribution of wood to the axial second moment of area ($I_{rel,wood}$) and structural bending modulus (E_{str}), (C) between wood density and structural bending modulus (E_{str}), and (D) between wood density and fibre double wall thickness to lumen diameter ratio. The symbols represent mean values and SD of roots (black) and stems (grey).

stiffness and storage capacity is clearly apparent between roots and self-supporting stems (Fig. 7A). The stems of the non-self-supporting liana *Clematis vitalba* exhibited low mechanical stiffness and high hydraulic conductivity, and hence clustered with roots (Figs 6, 7A). The stems of *Tilia cordata* were positioned in the centre of the ternary plot (Fig. 7A), exhibiting the strongest compromise between all three functions. When the data for *Clematis vitalba* were excluded and the data for self-supporting trees were plotted separately for roots (Fig. 7B) and stems (Fig. 7C), the within organ variation became more apparent. The root data (Fig. 7B) separated more homogeneously across the functional triangle compared with stems (Fig. 7C), in which the data were mostly positioned along the mechanics–storage trade-off. Within roots (Fig. 7B), hydraulics was the dominant function in *Robinia pseudoaccacia*, *Fraxinus excelsior*, and *Tilia cordata*, while mechanics was dominant in *Carpinus betulus* and *Fagus sylvatica*, with storage being dominant in *Quercus robur*. All three functions were most strongly compromised in the roots of *Acer pseudoplatanus* and *Prunus avium*. Within stems (Fig. 7C), the mechanical function was most pronounced in *Carpinus betulus* and *Prunus avium*, while the storage function was most dominant in *Quercus robur*, with hydraulics being most prominent in *Tilia cordata*. The stems of *Fraxiunus excelsior* compromised mainly between the mechanical and hydraulic function, while *Fagus sylvatica*, *Robinia pseudoaccacia*, and *Acer pseudoplatanus* were found to be compromised between storage and mechanical functions.

Discussion

In agreement with our hypothesis, roots showed lower resistance to both bending and twisting forces than self-supporting stems (Fig. 1A, B). From the two mechanical parameters, a greater difference was observed in E_{str} than in G_{str}, resulting in lower twist to bend ratios (EI/GI) of roots (Fig. 1C). The higher mechanical stiffness of self-supporting stems allows them to grow outward and support leaves for efficient light acquisition. Contrarily, the greater mechanical flexibility of roots helps them to avoid overcritical bending and torsional loads caused by the movement of soil components in relation to the Mohr–Coulomb law (Mattheck and Breloer, 1994), and allows roots to navigate their surroundings with less resistance. Mechanical properties of woody roots were less frequently quantified than those of stems, despite their importance in anchoring trees to their substrate (Niklas, 1999*b*; Karrenberg *et al.*, 2003), penetrating compacted soil (Day *et al.*, 1995), and stabilising and reinforcing slopes (Schwarz *et al.*, 2010). Thus, our data may be useful to parameterise models for these kinds of applications. However, it has to be taken into account that we did not investigate the variation of mechanical properties along the stems and roots depending on their position within the plant and their stage of ontogeny. Fine roots are likely to be exposed to tensile forces and show a high tensile rigidity, whereas older root segments close to the stem base show a high resistance to bending and compression (Ennos, 2000). In order to allow for a comparison between species we sampled all root segments at approximately 1 m from the root collar. It

Downloaded from https://academic.oup.com/jxb/article-abstract/70/14/3679/5531920 by Lib4RI Empa user on 03 September 2019

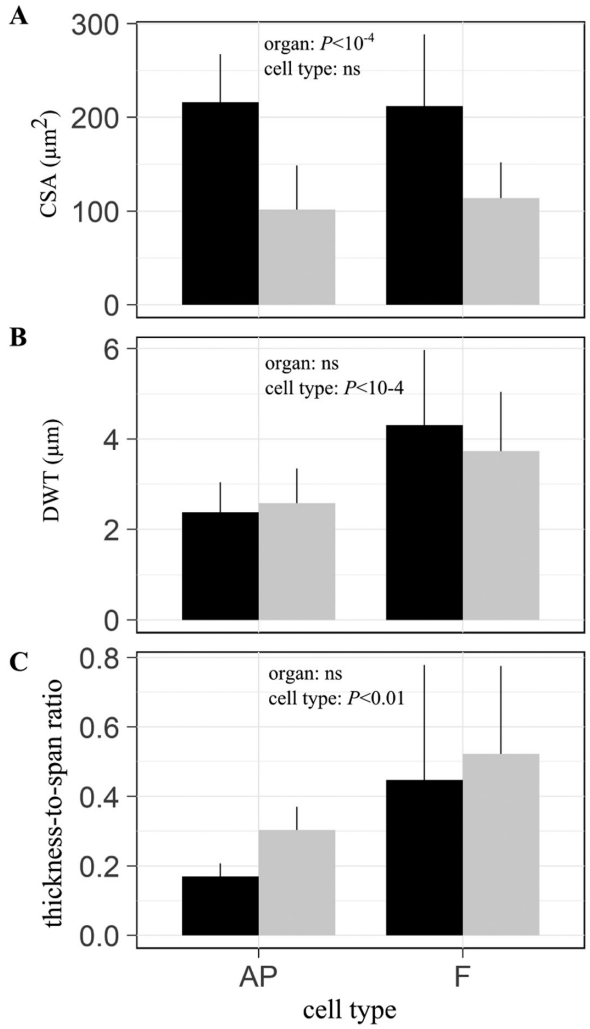

Fig. 3. Comparison of axial wood parenchyma and fibre cell structure in roots and stems of nine angiosperm species. Mean values and SD of (A) cell cross-sectional area (CSA), (B) double wall thickness (DWT), and (C) thickness to span ratio of axial wood parenchyma (AP) and fibre (F) cells. Roots and stems are depicted in black and grey, respectively. Significance levels for the fixed effect factors organ and cell type are given (mixed effect models with random effect of species).

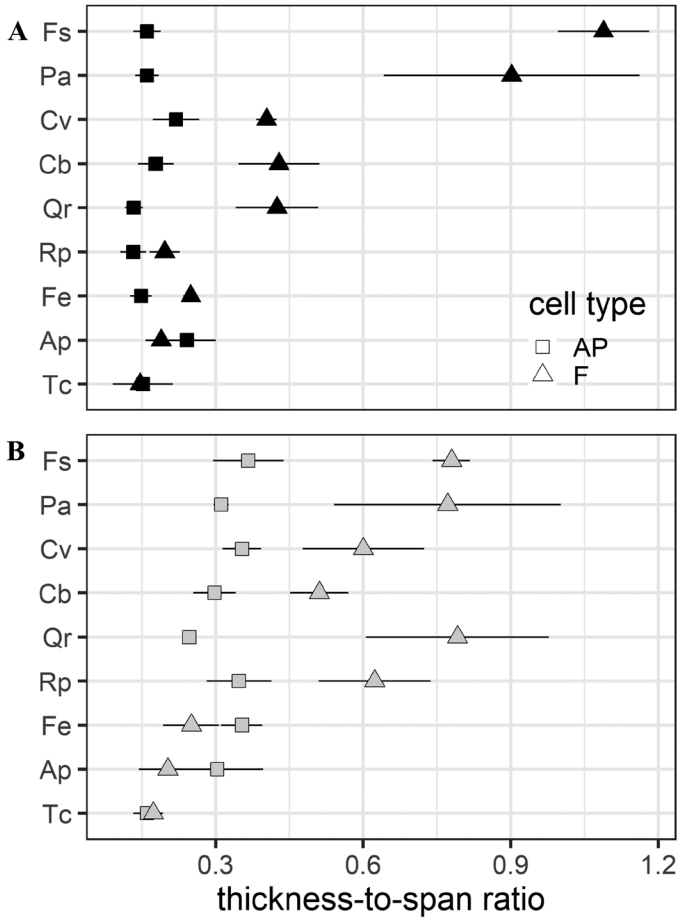

Fig. 4. Variation in thickness to span ratio (i.e. the ratio between double wall thickness and cell lumen diameter) of axial wood parenchyma cells (AP, black) and fibres (F, grey) in roots (A) and stems (B) of nine woody angiosperm species. For abbreviation of species names see Table 1.

is likely that segments farther away from the stem show different mechanical properties, in particular in tension, which we have not studied here. Young stems (or the young tips of stems) are also known to be more flexible in bending than older stems (or the older bases of stems) and are therefore able to avoid critical stresses by streamlining parallel to mechanical forces (e.g. when submitted to wind loads), whereas older stems have a considerably higher bending resistance (Speck, 1994; Speck *et al.*, 1996; Rowe and Speck, 2004).

The structural underpinnings of mechanical properties can be linked to multiple morpho-anatomical characteristics of woody organs (Figs 2, 6). In both woody organs, E_{str} and the G_{str} were positively correlated to a greater proportion of wood relative to bark. While wood represents the stronger of the two tissues, the importance of bark for whole organ mechanics originates mainly from its position far from the neutral axis (Niklas, 1999*a*; Karrenberg *et al.*, 2003). The overall lower $I_{rel,wood}$ and the relatively weaker correlation of $I_{rel,wood}$ with both structural moduli in roots compared with stems (Fig. 2B) indicates that the relative contribution of bark to the mechanical properties was greater in roots. These results are consistent with Pratt *et al.* (2007), who reported an important contribution of bark to root mechanics for nine chaparral species. In our study, higher values of $I_{rel,bark}$ were typically found in organs with low wood density (e.g. in the roots of *Robinia pseudoacacia*, *Fraxinus excelsior*, and *Quercus robur*, and in the stems of *Tilia cordata*) suggesting that a thick bark, sometimes strengthened by the presence of lignified fibres (Fig. 5C), partially compensates for a mechanically weak wood and may even have additional functions for controlling tree posture (Clair *et al.*, 2019). An additional structural role of bark may be in the protection from abrasion caused by soil particles and stones when roots are mechanically loaded. However, other functions, unrelated to mechanical properties, such as defence against pathogens, storage, and phloem transport towards the root apical meristems, are also correlated with bark thickness (Rosell *et al.*, 2014).

Although there was no significant difference in wood density between the tested young roots and stems, wood density was positively related to E_{str} and G_{str} across species (Fig. 2C). A close association of wood density and mechanical properties has also been evidenced in a number of previous studies (Jacobsen *et al.*,

Downloaded from https://academic.oup.com/jxb/article-abstract/70/14/3679/5531920 by Lib4RI Empa user on 03 September 2019

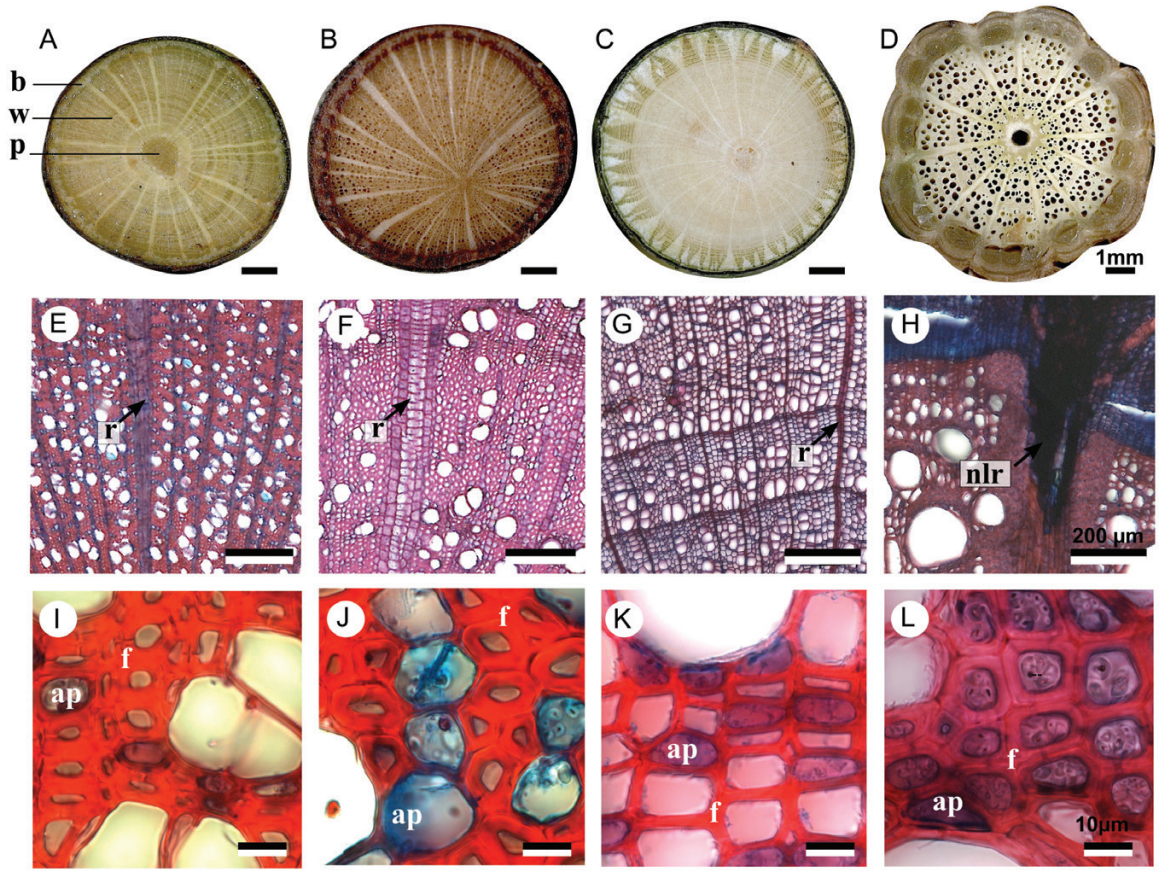

Fig. 5. Anatomy of young woody roots and stems at three different magnifications. Anatomical characteristics of roots of *Fagus sylvatica* (A, E, I) and stems of *Fagus sylvatica* (B, F, J), stems of *Tilia cordata* (C, G, K) and stems of *Clematis vitalba* (D, H, L) photographed at increasing magnification. Thicker bark (A versus B), wider rays (E versus F) and greater size of xylem cells (I versus J) are typical of roots compared with stems. Stems of *Tilia cordata* have a thick bark strengthened by strands of lignified fibres (C), wood of low density (G) and fibre and axial parenchyma with narrow cell walls (K). Specialized anatomy of lianescent stem of *Clematis vitalba* showing lobbed wood–bark boundary (D), wide multiseriate rays that have a non-lignified outermost portion (nlr-r) (H) and living fibres large in diameter and with a thick secondary wall (L). Abbreviations: ap, axial parenchyma; b, bark; f, fibre; nlr, non-lignified ray; p, pith; r, ray; w, wood.

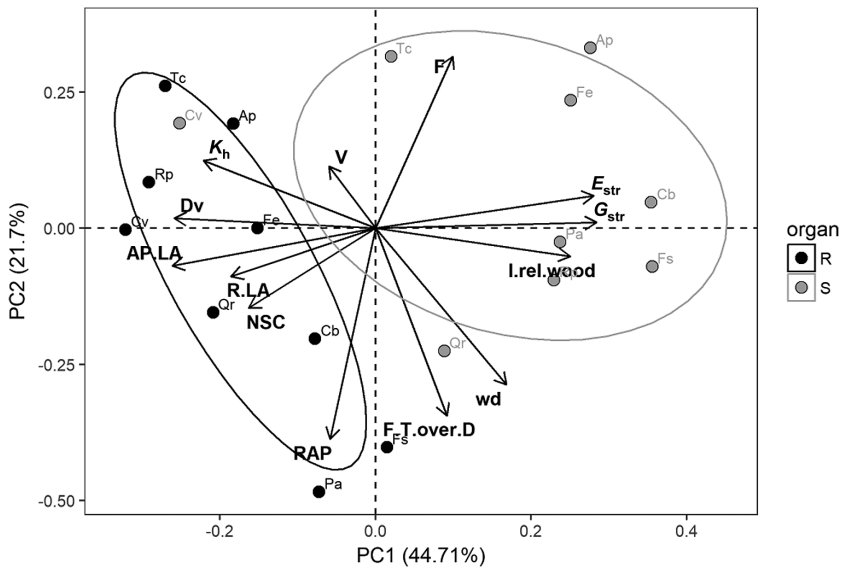

Fig. 6. Principal component analysis (PCA) biplot showing the overall coordination of xylem structural traits in roots (black) and stems (grey). Structural traits are lumen area of axial and ray parenchyma (AP.LA, R.LA), vessel diameter (Dv), thickness to span ratio of fibres (F.T.over.D), fibres tissue fraction (F), ray and axial parenchyma tissue fraction (RAP), vessel tissue fractions (V), theoretical hydraulic conductivity (K_h), concentration of non-structural carbohydrates (NSC), bending structural modulus (E_{str}), torsional structural moduls (G_{str}) and wood density (wd). Roots and stems are depicted in black and grey symbols, respectively. For abbreviation of species names see Table 1.

Downloaded from https://academic.oup.com/jxb/article-abstract/70/14/3679/5531920 by Lib4RI Empa user on 03 September 2019

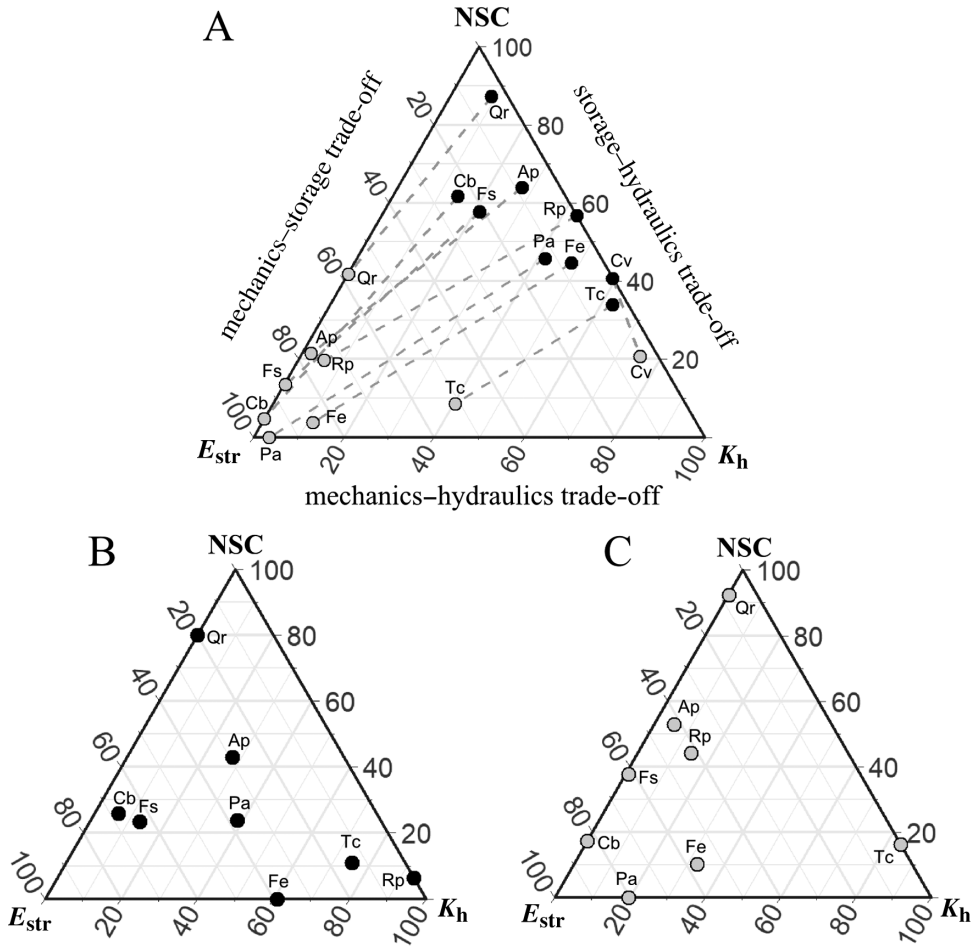

Fig. 7. Trade-off triangle showing the relative division of xylem function between mechanical stiffness, carbohydrate storage capacity, and hydraulic conductivity for roots and stems of nine woody angiosperm species. Data from both organs are plotted together (A), or for roots (B) and stems (C) separately. The data for non-self-supporting *Clematis vitalba* are not included in (B, C). Mechanical properties are represented by the structural bending modulus (E_{str}), storage capacity is represented by the concentration of non-structural carbohydrates measured at the onset of winter dormancy (NSC), and hydraulic conductivity is represented by the theoretical hydraulic conductivity (K_h). Species abbreviations follow Table 1. Roots and stems are shown in black and grey symbols, respectively.

2007; Chave *et al.*, 2009; Niklas and Spatz, 2010). From all anatomical parameters measured, wood density was most strongly correlated with the wall thickness to span ratio of fibres (Fig. 2D). Mechanically stiffer stems also had higher area fractions of fibres and lower fractions of ray and axial parenchyma compared with roots (Table 2). However, the higher fractions of parenchyma did not translate directly into reduced mechanical stiffness despite parenchyma cells having lower thickness to span ratios than fibres (Fig. 3C). The finding that fibre reinforcement rather than fibre proportions exerts major control over wood density and mechanical performance is in line with the findings on 24 Australian tree and shrub species from three climate zones (Ziemińska *et al.*, 2013).

Parenchyma and fibre cells were on average larger in diameter in roots than in stems, while the wall thickness did not differ significantly between organs (Fig. 3A, B). Consequently, the larger cell size resulted in lower thickness to span ratio of root fibres and axial wood parenchyma cells, which is in line with lower mechanical demands and greater storage capacity of roots. While the presence of narrower cell walls constitutes an important criterion in the formal anatomical definition of axial wood parenchyma cells (Wheeler *et al.*, 1989; Carlquist, 2001), our results demonstrate that the morphological dichotomy between fibres and axial parenchyma cells is highly variable across species (Figs 4, 5I–L). The dichotomy was large in *Fagus sylvatica* and *Prunus avium*, and low in *Acer pseudoplatanus*, *Fraxinus excelsior*, and *Tilia cordata*. The difference was mainly driven by fibre wall thickness, while the lumen size and wall thickness of axial parenchyma cells were rather uniform across species.

Due to its radial orientation, the effect of ray parenchyma on mechanical stiffness is complex and will differ depending on the direction of mechanical loading. In our study, a higher fraction of ray parenchyma associated with the presence of wider rays (Table 2) could contribute to a greater mechanical flexibility of roots compared with stems. Wide multiseriate rays were found in the roots of *Clematis vitalba*, *Fagus sylvatica* (Fig. 5A, E), and *Prunus avium*, and also in the stems of *Fagus sylvatica* (Fig. 5B, F). Ray cells in most of the tested species appeared fully lignified as suggested by a positive staining reaction with safranin, and the thickness of their walls was comparable to those of fibres. Only the rays of *Clematis vitalba* were partially non-lignified (Fig. 5H). In this climbing species, wide non-lignified

Downloaded from https://academic.oup.com/jxb/article-abstract/70/14/3679/5531920 by Lib4RI Empa user on 03 September 2019

Table 2. *Anatomical parameters of ray and axial parenchyma for roots and stems of nine woody angiosperm species*

Species	RP (%)	AP (%)	RAP (%)	Ray density (count per 90° wedge)	Ray width (μm)	AP DWT (μm)	AP D_L (μm)
Roots							
All	18.2±5.2a	13.0±6.3a	31.3±9.2a	24.4±11.1a	32.8±26.2a	2.4±0.7a	14.1±1.4a
Ap	14.7±6.4	0.7±0.3	15.4±6.6	22.3±7	17.3±3.3	3.4±0.3	14.3±2.5
Cb	20.3±3.8	15±2.6	35.3±6.4	36.3±3.5	30.3±6.4	2.6±0.6	14.3±0.8
Fe	13.2±3.9	21.1±3.3	34.3±4.2	20±4	19.5±6.2	2.2±0.3	14.9±1
Fs	23.1±9.5	17.1±6.9	40.2±8.2	21±1.7	43.2±2.1	2.1±0.4	13.1±0.4
Pa	28.8±3.5	14.3±2.3	43.1±5.2	33±5.6	35.7±11	2±0.1	12.5±1.5
Qr	18.9±1.5	16.9±8	35.7±7.5	39.7±13.1	15.9±1.9	1.8±0.1	13.9±1.5
Rp	17.1±2	15.5±1.3	32.6±2.5	28.3±7.1	16±0.2	2±0.4	15.4±0.3
Tc	15.6±3.8	5.4±2.1	21±4.5	13.7±3.8	19.6±5.3	1.8±0.5	12±1.6
Cv	12.5±5.3	11.3±3.6	23.8±8.6	5±1	97.5±2.8	3.6±0.3	16.6±2.1
Stems							
All	13.7±4.0b	8.8±7.6a	22.5±6.5b	30.7±12.2b	26.6±34.1a	2.6±0.8a	8.6±1.7b
Ap	11.5±5.1	1.8±0.6	13.4±5.7	30.3±2.1	10.2±1	2.5±0.5	8.6±1.2
Cb	17.6±2	6.2±2.7	23.8±0.8	49.3±9	11.2±1.1	2.7±0.4	9.1±0.3
Fe	13.3±4.5	5.4±0.4	18.7±4.8	25.3±4.9	13±1.4	2.7±0.3	7.5±0.2
Fs	16.4±0.4	30.7±5.3	47.1±5.7	20.7±1.2	21.1±2.9	1.6±0.2	21.1±1.9
Pa	20.7±3.5	2.7±1	23.4±4.5	41±3.6	13±1.7	2.1±0.2	6.6±0.4
Qr	10.9±2.1	22.7±2.1	33.6±0.1	35.3±4	9.9±1.4	2.2±0.2	9±1
Rp	9.9±1.6	20.9±6.3	30.8±7.8	30.3±6.7	11.1±2	2.7±0.4	7.9±0.5
Tc	9.7±0.7	7.5±2.3	17.2±2	27±5.3	11.3±1.3	1.5±0.4	9.4±0.9
Cv	12.1±3.7	6.1±3.3	18.3±3.4	5±1	111.3±8.5	4.3±0.3	12.4±1.7

Values represent means ±SD. Different letters indicate significant difference between roots and stems (mixed effect models with random effect of species). AP, area fraction of axial parenchyma; AP D_L, mean lumen diameter of axial parenchyma cells; AP DWT, mean double wall thickness of axial parenchyma cells; RAP, area fraction of ray and axial parenchyma; RP, area fraction of ray parenchyma.

portions of rays were present in the outermost region, close to the vascular cambium, thereby forming wedge-shaped incisions in the otherwise lignified secondary xylem. Due to their position far from the neutral axis, the incompletely lignified ray cells likely result in a substantial mechanical weakening and represent one of the structural features causing the high mechanical flexibility found in *Clematis vitalba* roots and stems (Isnard *et al.*, 2003). Similarly, non-lignified or partially lignified rays have also been observed in other climbers such as *Aristolochia malacophylla* (Wagner *et al.*, 2012). The high proportion of large-diameter vessels typical of lianescent wood and some roots can be considered as an additional factor contributing to the low mechanical stiffness in stems of climbing species (Gasson and Dobbins, 1991; Rowe and Speck, 1996, 2014; Gallenmüller *et al.*, 2001).

The overall structure–function trade-offs differ for between- and within-organ comparisons (Fig. 7). Our results demonstrate that it is rare for xylem to compromise all three functions equally. Instead, one of the three functions is usually more pronounced, while the remaining two functions may or may not co-vary. In self-supporting stems, the higher demands for mechanical stability clearly represent a major constraint. The isolated position of the stems of the liana *Clematis vitalba* in the trade-off triangle (Fig. 7) represents a further proof of the different mechanical and hydraulic properties of non-self-supporting plants (Rowe and Speck, 2004, 2014). In roots with fewer mechanical demands, xylem can be designed with a greater emphasis on either storage (e.g. *Quercus robur*) or hydraulic function (e.g. *Tilia cordata*, *Robina pseudoaccacia*; Fig. 7B).

The functional trade-offs primarily originate from a division of labour between different cell types. Besides cell type fractions, finer scale anatomical properties of different xylem cells, such as the lumen size and cell wall thickness, affect these relationships. From a functional perspective, the secondary wall thickness is critical in fibres, the lumen area in parenchyma cells and conduits (including vessels and tracheids). Our data show that, at least in juvenile wood, fibre wall thickness is highly variable across species and organs, while wall thickness of axial parenchyma is much less variable (Fig. 4). The main source of functional diversity in axial parenchyma across species is due to variation in their tissue fraction (Morris *et al.*, 2016*b*; Plavcová *et al.*, 2016), arrangement (Morris *et al.*, 2018), and biochemical properties (Plavcová and Jansen, 2015), rather than in the lumen size of individual cells. In contrast to axial parenchyma cells, vessel diameter is greatly variable across species and organs (Hacke *et al.*, 2017). Greater plasticity of vessel diameter may represent a selective advantage because hydraulic function is more sensitive to increases in vessel diameter. In accordance with the Hagen–Poiseuille equation, even a small increase in vessel diameter results in a large increase in conductivity, depending on the vessel diameter by the power of four (Tyree and Ewers, 1991). However, in self-supporting species the xylem structure is not severely altered by conduit width because larger conduits are less numerous, and the overall conduit lumen fraction remains fairly similar at around 15–20% (Zanne *et al.*, 2010; Morris *et al.*, 2016*b*).

In summary, our results demonstrate that higher demands for mechanical stability in self-supporting stems put a major

Downloaded from https://academic.oup.com/jxb/article-abstract/70/14/3679/5531920 by Lib4RI Empa user on 03 September 2019

constraint on xylem structure, whereas root xylem can be designed with a greater emphasis on both storage and hydraulic functions. The interplay between mechanical stiffness, nutrient storage, and hydraulic conductivity in young woody roots and stems is driven by differences in cell type relative fractions, cell size, and secondary wall reinforcement of these cells.

Acknowledgements

LP was initially supported by a Postdoctoral Fellowship from the Alexander von Humboldt Foundation and research funding granted by Ulm University and Ulm University Society (Ulmer Universitätsgesellschaft). SJ acknowledges the German Research Foundation (DFG, project no. JA 2174/3-1) for financial support. We wish to thank the Botanical Garden of the University of Freiburg for access to plant material. We also thank Jan Plavec and Aneta Bulíčková for technical assistance and Dr Stephanie Stuart for useful discussions.

References

Baas P, Ewers FW, Davis SD, Wheeler EA. 2004. Evolution of xylem physiology. In: Hemsley AR, Poole I, eds. The evolution of plant physiology. London: Elsevier Academic Press, 273–295.

Badel E, Ewers FW, Cochard H, Telewski FW. 2015. Acclimation of mechanical and hydraulic functions in trees: impact of the thigmomorphogenetic process. Frontiers in Plant Science **6**, 266.

Bittencourt PR, Pereira L, Oliveira RS. 2016. On xylem hydraulic efficiencies, wood space-use and the safety-efficiency tradeoff: comment on Gleason *et al*. (2016) 'Weak tradeoff between xylem safety and xylem-specific hydraulic efficiency across the world's woody plant species'. New Phytologist **211**, 1152–1155.

Brodersen CR, McElrone AJ, Choat B, Matthews MA, Shackel KA. 2010. The dynamics of embolism repair in xylem: in vivo visualizations using high-resolution computed tomography. Plant Physiology **154**, 1088–1095.

Burgert I, Bernasconi A, Niklas K, Eckstein D. 2001. The influence of rays on the transverse elastic anisotropy in green wood of deciduous trees. Holzforschung **55**, 449–454.

Cai J, Li S, Zhang H, Zhang S, Tyree MT. 2014. Recalcitrant vulnerability curves: methods of analysis and the concept of fibre bridges for enhanced cavitation resistance. Plant, Cell & Environment **37**, 35–44.

Carlquist S. 2001. Comparative wood anatomy: systematic, ecological, and evolutionary aspects of dicotyledon wood. Berlin, Heidelberg: Springer-Verlag.

Chave J, Coomes D, Jansen S, Lewis SL, Swenson NG, Zanne AE. 2009. Towards a worldwide wood economics spectrum. Ecology Letters **12**, 351–366.

Christensen-Dalsgaard KK, Ennos AR, Fournier M. 2007*a*. Changes in hydraulic conductivity, mechanical properties, and density reflecting the fall in strain along the lateral roots of two species of tropical trees. Journal of Experimental Botany **58**, 4095–4105.

Christensen-Dalsgaard KK, Fournier M, Ennos AR, Barfod AS. 2007*b*. Changes in vessel anatomy in response to mechanical loading in six species of tropical trees. New Phytologist **176**, 610–622.

Clair B, Ghislain B, Prunier J, Lehnebach R, Beauchêne J, Alméras T. 2019. Mechanical contribution of secondary phloem to postural control in trees: the bark side of the force. New Phytologist **221**, 209–217.

Day S, Bassuk N, Van Es H. 1995. Effects of four compaction remediation methods for landscape trees on soil aeration, mechanical impedance and tree establishment. Journal of Environmental Horticulture **13**, 64–64.

Ennos, AR. 2000. The mechanics of root anchorage. Advances in Botanical Research **33**, 133–157.

Fujiwara S. 1992. Anatomy and properties of Japanese hardwoods II. Variation of dimensions of ray cells and their relation to basic density. IAWA Bulletin **13**, 397–402.

Fujiwara S, Sameshima K, Kuroda K, Takamura N. 1991. Anatomy and properties of Japanese hardwoods. I. Variation of fibre dimensions and tissue proportions and their relation to basic density. IAWA Bulletin **12**, 419–424.

Gallenmüller F, Müller U, Rowe N, Speck T. 2001. The growth form of *Croton pullei* (Euphorbiaceae) – functional morphology and biomechanics of a neotropical liana. Plant Biology **3**, 50–61.

Gartner BL. 1991. Stem hydraulic properties of vines vs. shrubs of western poison oak, *Toxicodendron diversilobum*. Oecologia **87**, 180–189.

Gasson P, Dobbins DR. 1991. Wood anatomy of the Bignoniaceae, with a comparison of trees and lianas. IAWA Bulletin **12**, 389–417.

Gleason SM, Westoby M, Jansen S, *et al*. 2016. Weak tradeoff between xylem safety and xylem-specific hydraulic efficiency across the world's woody plant species. New Phytologist **209**, 123–136.

Hacke UG, Spicer R, Schreiber SG, Plavcová L. 2017. An ecophysiological and developmental perspective on variation in vessel diameter. Plant, Cell & Environment **40**, 831–845.

Hamilton NE, Ferry M. 2018. *ggtern*: ternary diagrams using ggplot2. Journal of Statistical Software, Code Snippets **87**, 1–17.

Isnard S, Speck T, Rowe N. 2003. Mechanical architecture and development in *Clematis*: implications for canalised evolution of growth forms. New Phytologist **158**, 543–559.

Jacobsen AL, Agenbag L, Esler KJ, Pratt RB, Ewers FW, Davis SD. 2007. Xylem density, biomechanics and anatomical traits correlate with water stress in 17 evergreen shrub species of the Mediterranean-type climate region of South Africa. Journal of Ecology **95**, 171–183.

Jacobsen AL, Ewers FW, Pratt RB, Paddock WA 3rd, Davis SD. 2005. Do xylem fibers affect vessel cavitation resistance? Plant Physiology **139**, 546–556.

Jupa R, Plavcová L, Gloser V, Jansen S. 2016. Linking xylem water storage with anatomical parameters in five temperate tree species. Tree Physiology **36**, 756–769.

Karrenberg S, Blaser S, Kollmann J, Speck T, Edwards P. 2003. Root anchorage of saplings and cuttings of woody pioneer species in a riparian environment. Functional Ecology **17**, 170–177.

Lachenbruch B, McCulloh KA. 2014. Traits, properties, and performance: how woody plants combine hydraulic and mechanical functions in a cell, tissue, or whole plant. New Phytologist **204**, 747–764.

Lens F, Picon-Cochard C, Delmas CE, *et al*. 2016. Herbaceous angiosperms are not more vulnerable to drought-induced embolism than Angiosperm trees. Plant Physiology **172**, 661–667.

Lens F, Sperry JS, Christman MA, Choat B, Rabaey D, Jansen S. 2011. Testing hypotheses that link wood anatomy to cavitation resistance and hydraulic conductivity in the genus *Acer*. New Phytologist **190**, 709–723.

Mattheck C, Breloer H. 1994. The body language of trees: a handbook for failure analysis [Edited by David Lonsdale from a translation by Robert Strouts]. London: H. M. Stationery Office.

McCulloh K, Sperry JS, Lachenbruch B, Meinzer FC, Reich PB, Voelker S. 2010. Moving water well: comparing hydraulic efficiency in twigs and trunks of coniferous, ring-porous, and diffuse-porous saplings from temperate and tropical forests. New Phytologist **186**, 439–450.

Morris H, Brodersen C, Schwarze FW, Jansen S. 2016*a*. The parenchyma of secondary xylem and its critical role in tree defense against fungal decay in relation to the CODIT model. Frontiers in Plant Science **7**, 1665.

Morris H, Gillingham MAF, Plavcová L, *et al*. 2018. Vessel diameter is related to amount and spatial arrangement of axial parenchyma in woody angiosperms. Plant, Cell & Environment **41**, 245–260.

Morris H, Plavcová L, Cvecko P, *et al*. 2016*b*. A global analysis of parenchyma tissue fractions in secondary xylem of seed plants. New Phytologist **209**, 1553–1565.

Niklas KJ. 1992. Plant biomechanics: an engineering approach to plant form and function. Chicago: University of Chicago Press.

Niklas KJ. 1999*a*. The mechanical role of bark. American Journal of Botany **86**, 465–469.

Niklas KJ. 1999*b*. Variations of the mechanical properties of *Acer saccharum* roots. Journal of Experimental Botany **50**, 193–200.

Downloaded from https://academic.oup.com/jxb/article-abstract/70/14/3679/5531920 by Lib4RI Empa user on 03 September 2019

Niklas KJ, Spatz H-C. 2010. Worldwide correlations of mechanical properties and green wood density. American Journal of Botany **97**, 1587–1594.

Pfautsch S, Hölttä T, Mencuccini M. 2015. Hydraulic functioning of tree stems—fusing ray anatomy, radial transfer and capacitance. Tree Physiology, **35**, 706–722.

Pinheiro J, Bates D, DebRoy S, Sarkar D, **The R Development Core Team**. 2013. nlme: linear and nonlinear mixed effects models. R package version 3.1-108.

Pittermann J, Sperry JS, Wheeler JK, Hacke UG, Sikkema EH. 2006. Mechanical reinforcement of tracheids compromises the hydraulic efficiency of conifer xylem. Plant, Cell & Environment **29**, 1618–1628.

Plavcová L, Hoch G, Morris H, Ghiasi S, Jansen S. 2016. The amount of parenchyma and living fibers affects storage of nonstructural carbohydrates in young stems and roots of temperate trees. American Journal of Botany **103**, 603–612.

Plavcová L, Jansen S. 2015. The role of xylem parenchyma in the storage and utilization of nonstructural carbohydrates. In: Hacke UG, ed. Functional and ecological xylem anatomy. Cham: Springer International Publishing, 209–234.

Pratt RB, Jacobsen AL. 2017. Conflicting demands on angiosperm xylem: Tradeoffs among storage, transport and biomechanics. Plant, Cell & Environment **40**, 897–913.

Pratt RB, Jacobsen AL, Ewers FW, Davis SD. 2007. Relationships among xylem transport, biomechanics and storage in stems and roots of nine Rhamnaceae species of the California chaparral. New Phytologist **174**, 787–798.

Putz FE, Holbrook NM. 1991. Biomechanical studies of vines. In Putz FE, Mooney HA, eds. The biology of vines. Cambridge: Cambridge University Press, 73–98.

R Core Team. 2016. R: a language and environment for statistical computing. Vienna, Austria: R Foundation for Statistical Computing. https://www.R-project.org/.

Rosell JA, Gleason S, Méndez-Alonzo R, Chang Y, Westoby M. 2014. Bark functional ecology: evidence for tradeoffs, functional coordination, and environment producing bark diversity. New Phytologist **201**, 486–497.

Rowe NP, Isnard S, Gallenmüller F, Speck T. 2006. Diversity of mechanical architectures in climbing plants: an ecological perspective. In: Herrel A, Speck T, Rowe NP, eds. Ecology and biomechanics: a mechanical approach to the ecology of animals and plants. Boca Raton, FL, USA: Taylor & Francis, 35–59.

Rowe NP, Speck T. 1996. Biomechanical characteristics of the ontogeny and growth habit of the tropical liana *Condylocarpon guianense* (Apocynaceae). International Journal of Plant Sciences **157**, 406–417.

Rowe N, Speck T. 2004. Hydraulics and mechanics of plants: novelty, innovation and evolution. In: Hamsley AR, Poole I, eds. The evolution of plant physiology. London: Elsevier Academic Press, 297–325.

Rowe NP, Speck T. 2014. Stem biomechanics, strength of attachment, and developmental plasticity of vines and lianas. In: Schnitzer S, Bongers F, Burnham, R, Putz F, eds. Ecology of lianas. Chichester: Wiley-Blackwell, 323–341.

Schindelin J, Arganda-Carreras I, Frise E, *et al*. 2012. Fiji: an open-source platform for biological-image analysis. Nature Methods **9**, 676–682.

Schwarz M, Cohen D, Or D. 2010. Root-soil mechanical interactions during pullout and failure of root bundles. Journal of Geophysical Research: Earth Surface **115**, F04035.

Speck T. 1994. Bending stability of plant stems: ontogenetical, ecological, and phylogenetical aspects. Biomimetics **2**, 109–128.

Speck T, Burgert I. 2011. Plant stems: functional design and mechanics. Annual Review of Materials Research **41**, 169–193.

Speck T, Rowe NP, Bruechert F, Haberer W, Gallenmüller F, Spatz H-C. 1996. How plants adjust the'material properties' of their stems according to differing mechanical constraints during growth: an example of smart design in nature. In: The 3rd Biennial Joint Conference on Engineering Systems Design and Analysis, ESDA. Part 5, 233–241.

Tyree MT, Ewers FW. 1991. The hydraulic architecture of trees and other woody plants. New Phytologist **119**, 345–360.

Tyree MT, Yang S. 1990. Water-storage capacity of *Thuja*, *Tsuga* and *Acer* stems measured by dehydration isotherms: the contribution of capillary water and cavitation. Planta **182**, 420–426.

van der Sande MT, Poorter L, Schnitzer SA, Engelbrecht BMJ, Markesteijn L. 2019. The hydraulic efficiency-safety trade-off differs between lianas and trees. Ecology **100**, e02666.

Wagner ST, Isnard S, Rowe NP, Samain MS, Neinhuis C, Wanke S. 2012. Escaping the lianoid habit: evolution of shrub-like growth forms in *Aristolochia* subgenus *Isotrema* (Aristolochiaceae). American Journal of Botany **99**, 1609–1629.

Wheeler EA, Baas P, Gasson PE. 1989. IAWA list of microscopic features for hardwood identification. IAWA Bulletin **10**, 219–332.

Woodrum CL, Ewers FW, Telewski FW. 2003. Hydraulic, biomechanical, and anatomical interactions of xylem from five species of *Acer* (Aceraceae). American Journal of Botany **90**, 693–699.

Yamada Y, Awano T, Fujita M, Takabe K. 2011. Living wood fibers act as large-capacity "single-use" starch storage in black locust (*Robinia pseudoacacia*). Trees **25**, 607–616.

Zanne AE, Westoby M, Falster DS, Ackerly DD, Loarie SR, Arnold SE, Coomes DA. 2010. Angiosperm wood structure: global patterns in vessel anatomy and their relation to wood density and potential conductivity. American Journal of Botany **97**, 207–215.

Zheng J, Martínez-Cabrera HI. 2013. Wood anatomical correlates with theoretical conductivity and wood density across China: evolutionary evidence of the functional differentiation of axial and radial parenchyma. Annals of Botany **112**, 927–935.

Ziemińska K, Butler DW, Gleason SM, Wright IJ, Westoby M. 2013. Fibre wall and lumen fractions drive wood density variation across 24 Australian angiosperms. AoB Plants **5**, plt046.

Ziemińska K, Westoby M, Wright IJ. 2015. Correction: broad anatomical variation within a narrow wood density range-a study of twig wood across 69 Australian angiosperms. PLoS ONE **10**, e0139496.

Downloaded from https://academic.oup.com/jxb/article-abstract/70/14/3679/5531920 by Lib4RI Empa user on 03 September 2019